

Oscillating bubbles in teardrop cavities for microflow control

Ali Hashmi · Garrett Heiman · Gan Yu ·
Mark Lewis · Hyuck-Jin Kwon · Jie Xu

Received: 27 June 2012 / Accepted: 7 October 2012 / Published online: 23 October 2012
© Springer-Verlag Berlin Heidelberg 2012

Abstract Microstreaming generated from oscillating microbubbles has great potential in microfluidic applications for localized flow control. In this study, we explore the use of teardrop-shaped cavities for trapping microbubbles. Upon acoustic actuation, these microbubbles confined in teardrop cavities can be utilized to generate a directional microstreaming flow. We further show that by altering the acoustic excitation frequency, a flow-switch for altering flow direction in microfluidic environments can be achieved using two oppositely arranged teardrop cavities with different sizes. In the end, we show that an array of such bubble-filled teardrop cavities can act as a fixated microfluidic transport system allowing for on-chip particle manipulation in complex flow patterns. This inexpensive method to create flows to switch and transport elements based on teardrop cavities can be widely employed for microfluidic applications such as drug delivery systems.

Keywords Teardrop cavities · Microfluidics · Oscillating bubbles · Microflow · Acoustic actuation

A. Hashmi and G. Heiman equally contributed to this work.

Electronic supplementary material The online version of this article (doi:10.1007/s10404-012-1077-5) contains supplementary material, which is available to authorized users.

A. Hashmi · G. Heiman · G. Yu · M. Lewis · H.-J. Kwon ·
J. Xu (✉)
Department of Mechanical Engineering, Washington State
University, Vancouver, WA 98686, USA
e-mail: jie.xu@wsu.edu
URL: <http://research.vancouver.wsu.edu/microfluidics-lab>

1 Introduction

Efficient flow control (Stone et al. 2004; Garty et al. 2011) and particle handling (Wang and Zhe 2011; Yu et al. 2011; Xu and Attinger 2008) are the most quintessential tasks for lab-on-a-chip devices. Although still in their infancy, oscillating bubbles are rapidly proving to be a promising tool for addressing these critical issues (Hashmi et al. 2012a): in the recent decade, oscillating bubbles have been utilized for flow control as microfluidic pumps (Tovar et al. 2011) and mixers (Liu et al. 2002; Ahmed et al. 2009a, b; Wang et al. 2011b); for particle handling as tweezers (Chung and Cho 2008, 2009; Kwon et al. 2011; Lee et al. 2011), for manipulating biological organisms (Hashmi et al. 2012b), as fixated transporters (Marmottant and Hilgenfeldt 2004; Marmottant et al. 2006), filter (Rogers and Neild 2011), microrotors (Kao et al. 2007; Wang et al. 2006), propeller (Won et al. 2011), microfluidic switches (Patel et al. 2012; Wang et al. 2011a); and for expediting mass transfer across lipid bilayer membranes as remote surgeons for cell lysis (Marmottant and Hilgenfeldt 2003) and capsules to aid in the delivery of drugs and genes (Okabe et al. 2012; Hettiarachchi and Lee 2010; Hettiarachchi et al. 2009).

A bubble can be made to undergo oscillations via mechanical perturbations upon which beautiful flow patterns known as microstreaming result (Elder 1959). This second-order non-linear dynamical system is thought to exist due to a difference between the radial and the translational motion of the bubble (Marmottant and Hilgenfeldt 2003). Microstreaming flow field can be described as

$$u_i^{(b)} = u_o \sin(\Delta\varphi) \left[\frac{1}{2} S_{iz}^w - \frac{1}{4} M_{iz}^{D,w} - \frac{1}{2} M_{iz}^{H,w} \right] \quad (1)$$

where u_o is the streaming velocity of the bubble, $\Delta\varphi$ is the phase shift between the radial and the translational

components of the bubble's motion. The three terms within the square brackets starting from the left to the right are the dimensionless Green's function representing point force, dipole moment and the hexadecapole singularities at the center of an oscillating bubble attached to a wall. The far-field characteristics of the flow are dominated by the point force singularity, approximated by

$$u_{r \rightarrow \infty}^b = 6u_0 \frac{h_b^2}{a^2} \sin(\Delta\varphi) \frac{a^3}{r^3} \cos\theta \cos(2\theta) \quad (2)$$

where h_b is the standoff distance of the bubble center to the wall, a denotes the bubble radius, r is the radial distance away from the bubble center, and θ is the angle with the axis of translation or gravity. As can be seen from the equation the flow decays fast by a factor of $(1/r^3)$ away from the bubble center.

A popular way of generating microbubbles in microfluidics is by trapping gas into pre-fabricated micro-cavities (Xie et al. 2012; Huang et al. 2012; Patel et al. 2012; Tovar et al. 2011). These cavities are often symmetric in geometry, thus resulting in symmetric microstreaming patterns upon acoustic actuation. In this study, we explore for the first time the trapping behaviour of bubbles in asymmetrical cavities—teardrop-shaped cavities. We also explore the acoustic response of these trapped bubbles and their potential applications in microflow control.

2 Material, fabrication and methods

2.1 Micromilling

We use a micromilling machine (Minitch, CNC Mini-Mill/3 PRO, with a resolution of $0.8 \mu\text{m}$) for creating teardrop-shaped cavities in a polymethyl methacrylate (PMMA) chip to capture air-bubbles. Micromilling is adopted since it is both faster and more convenient than standard soft-lithography and does not require preparation

of a mask each time. Furthermore, micromilling allows us to fabricate holes with variously sized depths conveniently, which were confirmed using an optical measuring device (Quadra-Chek 200, with a spatial resolution of $1 \mu\text{m}$). PMMA was selected due to its transparency and the ease with which it can be milled. Initially cylindrical cavities with varying depths (50 , 40 and $30 \mu\text{m}$) were milled, and then a flow symmetry breaker was created by slightly modifying the hole morphology, i.e., making them teardrop shaped by introducing a tail (Fig. 1). In our experiments, we observed that the capability of the teardrop cavities to capture air bubbles relied heavily on the geometry of the cavity.

2.2 Cavity optimization for bubble trapping

We explored the effects of geometry on the bubble trapping behaviour. Three parameters were taken into account: the main hole depth D_h , the tail depth D_t and the tail length L_o (refer to Table 1 and Fig. 1c). The tail width was fixed at $76.2 \mu\text{m}$, contingent upon the size of the milling bit, and the main hole diameter was also a constant $120 \mu\text{m}$ for this set of experiments.

In the experiments, we observed that a progressively larger hole depth helped increase the success rate in trapping air bubbles. However, holes with depths deeper than $50 \mu\text{m}$ were not considered since greater depths highly increased the risk of mill bit breakages, and also because $50 \mu\text{m}$ hole depth already yielded a high success rate of confining bubbles within the main hole of the cavity. Moreover, we observed that if the ratio of D_h/D_t is small, then the air bubble surface is likely to cover the tail region of the cavity. In our later experiments, we found that this condition is not preferred due to its weak response to acoustic excitation. Therefore, the optimization goal was done to attain the best configuration that could enable us to capture air bubbles in the main hole without filling up the tail region (such as Fig. 1b). This is possible because the

Fig. 1 **a** Top view of two different sizes of teardrop-shaped cavities with trapped bubbles; **b** 3D view of a trapped bubble; **c** Schematic of a $120 \mu\text{m}$ teardrop cavity—the top view and the side view. The tail width is kept at $76.2 \mu\text{m}$ for all tested cavities. The hole depth (D_h), tail depth (D_t) and tail length (L_o) varied in the experiments

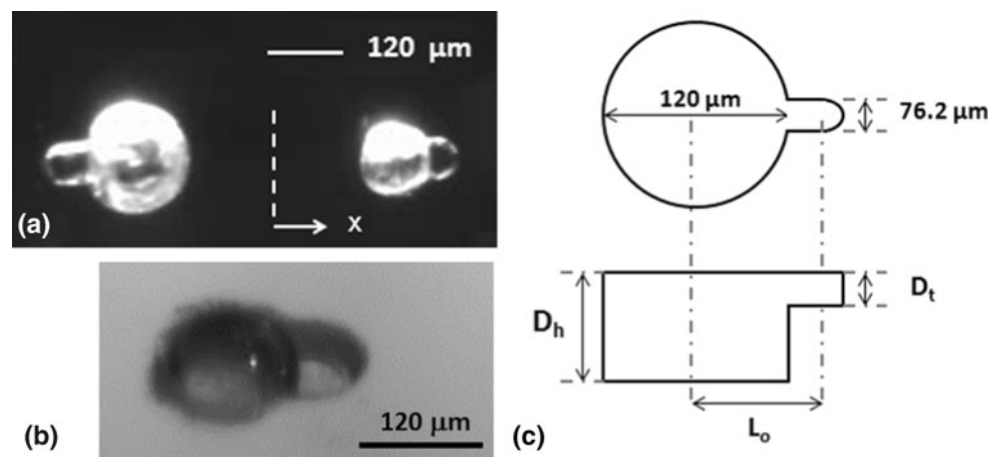


Table 1 The different cavity conditions tested for the optimum teardrop cavity configuration for trapping air bubbles

Geometry ID	Hole depth (D_h) (μm)	Tail length (L_o) (μm)	Tail depth (D_t) (μm)
1–9	50	60,80,100	10,20,30
10–18	40	60,80,100	10,20,30
19–27	30	60,80,100	10,20,30

bubbles always tend to minimize their surface energy by reducing the surface area. From our results (see Supplementary Material Figure S1) it can be deduced that cavities with a greater hole depth as well as a higher D_h/D_t were more efficient at trapping bubbles at the main hole and were featured in our later studies.

2.3 Experimental setup

The sketch of the experimental setup is shown in Fig. 2; the apparatus for conducting the experiments is a simple one: a piezoelectric actuator (HF-28/2 MC, Huifeng Piezoelectric Co. Ltd) is attached to one side of the PMMA chip using ultrasonic transmission gel (Aquasonic 100, Parker Laboratories, Inc). A function generator (DG1022, Rigol) and an amplifier (7602 M, Krohn-Hite, with a ± 0.5 V accuracy in the output peak voltage at 1 kHz) are used to input sinusoidal wave signals to the piezoelectric transducer at different frequencies to actuate the microbubbles trapped within the teardrop-shaped cavities. For our experiments, the top view of the cavities is monitored and captured using a high-speed camera (PixeLINK, PLB771U). Air bubbles are simply trapped within the holes by gently placing a de-ionized water droplet on top of them. Furthermore, microparticles of diameter 19 μm (Copolymer Microsphere Suspension, Thermo Scientific) are added to demonstrate particle transportation as well as

to indicate flow direction generated around the cavities during the experiments.

3 Results and discussion

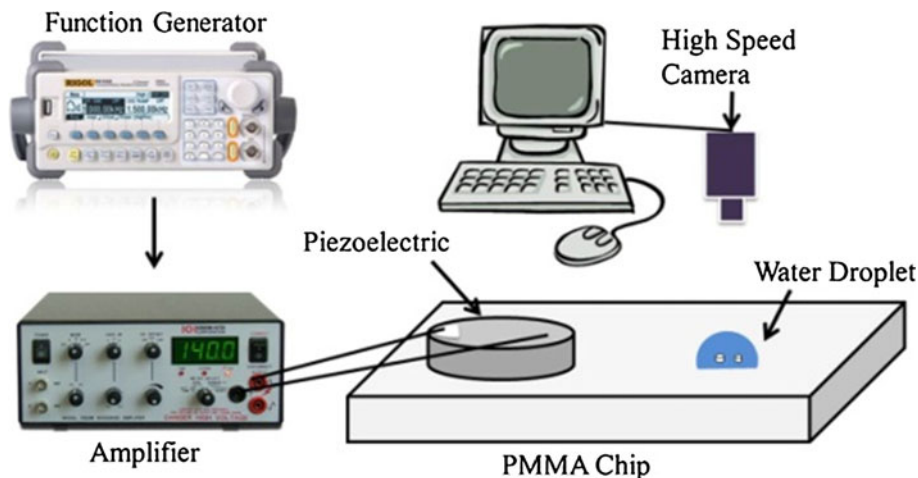
3.1 Directional microstreaming flow

Upon acoustic actuation of trapped microbubbles in the teardrop-shaped cavities we observed bubble oscillations resulting in a directed flow pattern rather than the traditional symmetric microstreaming (as shown in Fig. 3). We postulate that the presence of a tail around the trapped bubble breaks flow symmetry and induces a secondary flow around the bubble. This hypothesis is based on the previous study of Marmottant and Hilgenfeldt (2004), who reported that the presence of a particle in the vicinity of an oscillating bubble has the potential to induce a secondary flow around the particle, which in effect influences the flow-field around the bubble. However, detailed analytical solution of the flow field around our teardrop-shaped cavities is complex at this stage because of the complex geometries involved. Moreover, numerical simulation of the microstreaming flow is also challenging, due to the multiple spatial and temporal scales involved (Packer et al. 2008). On the other hand, surface wave (Xu and Attinger 2007a) and the shape oscillations of the bubbles (Matsumoto and Ueno 2009) are also important factors that require in-depth investigation in the future.

3.2 Frequency-selective flow switch

Precise temporal flow control is a fundamental challenge in microfluidics. Previously, passive frequency-selective flow control has been realized using complex microfluidic circuits (Leslie et al. 2009). Based on the teardrop-shaped cavity induced directional microstreaming flow, we

Fig. 2 Experimental setup: a piezoelectric actuator driven by electric signals is used to acoustically actuate air bubbles trapped within the teardrop cavities. A high-speed camera is used to record the experiments from the top



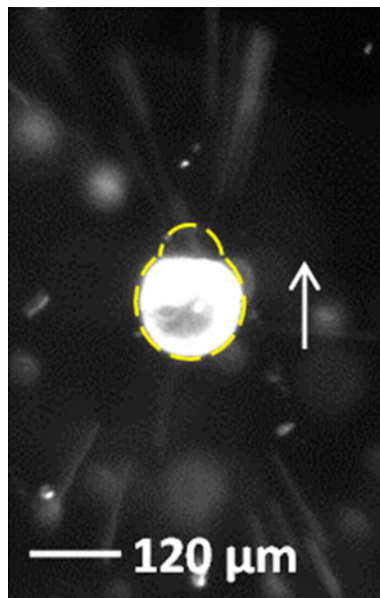


Fig. 3 Flow-field around an oscillating bubble trapped in the teardrop-shaped cavity captured at an exposure time of 190 ms. Arrow represents the direction of flow of microparticles

developed for the first time an active frequency-selective flow switch. Two oppositely facing teardrop-shaped cavities were constructed with size 120- and 200- μm to achieve selective acoustic actuation/response (refer to Fig. 1a).

Experiments were performed first selectively actuating the 120- μm bubble at 32 kHz and later selectively actuating the 200- μm bubble at 24 kHz. For the smaller sized bubble, particles are directed along the positive x -axis, whereas, they are forced to move the opposite direction when the larger bubble is actuated. The results of the velocity field around the bubble are presented in Fig. 4. The velocity field was mapped by tracing the trajectory of a seeded microparticle as it approached the bubble, accelerated and shot past the bubble while maintaining its motion on the symmetry line of the teardrop-shaped cavity. Nevertheless, a significant error is introduced while using this approach because of insufficient spatial and temporal resolutions. The error in particle position is quantified as the difference between the position where the particle assumes average velocity and the lower bound position, whereas an error in particle's velocity (Δv) is quantified as (Xu and Attinger 2007b)

$$\Delta v = \sqrt{\left(\frac{\delta}{dt}\right)^2 + \left(\frac{l\Delta t}{dt^2}\right)^2} \quad (4)$$

where δ is the error in particle position, dt is the time it takes for the particle to travel distance l and Δt is the half of the temporal resolution. Note that the temporal and spatial resolution strongly depends on the flow velocity, the defined frame-rate and the exposure time of each frame. In our

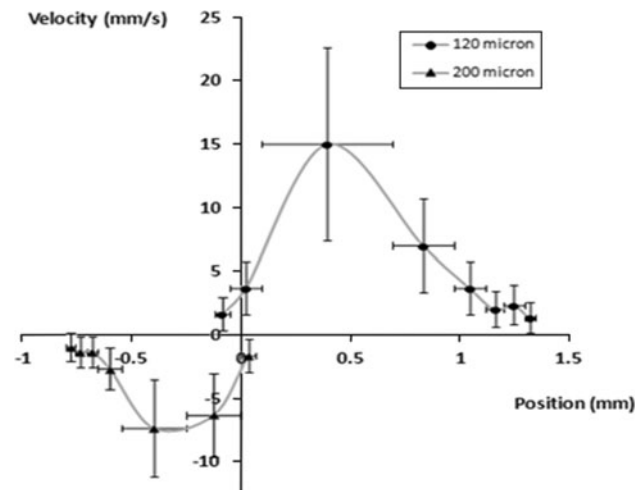


Fig. 4 Velocity of a microparticle as it approaches and leaves the teardrop-shaped cavity. The velocity of the particle is mapped by tracking the particles in the flow. Frequencies of 32 and 24 kHz were used for the 120- and 200-micron bubbles, respectively

experiments, $dt = 1/25$ s, $\Delta t = 1/50$ s and δ is conservatively estimated to be 40 μm . In the future, we hope to use more accurate techniques like the micro-Particle Image Velocimetry (μPIV) for reducing errors. However, at present the purpose is to demonstrate the flow switching mechanism and present a qualitative description of the flow. It is hoped that such a flow switch could be utilized for controlling the direction of flow as well as enhancing transport of particulate matter in microchannels in lab-on-a-chip devices.

3.3 Flow pattern control

Precise spatial flow control is another fundamental challenge in microfluidics. Here, we demonstrate that complex flow patterns can be constructed by chaining directional microstreaming flow using teardrop-shaped cavities in a certain arrangement, such as a square array with the tails pointing orthogonally to each other (Fig. 5 and Figure S2). Particles in the vicinity of the array were noticed to move in a butterfly-shaped pattern (clockwise) in accordance with the direction of the tails, forming a closed loop (see also supplementary movie). Furthermore, we observed that particles moving along the streamlines (symmetry lines of the teardrop-shaped cavities) move faster than the particles outside the loop. We can control the flow speed by tuning the input voltage that is applied to the piezo-actuator, and Fig. 6 plots the time a particle took to follow the loop (along the symmetry lines of the cavities) versus the input voltage.

3.4 Experimental repeatability

Experiments with the teardrop-shaped cavities showed a generally high repeatability in all cases, performing as

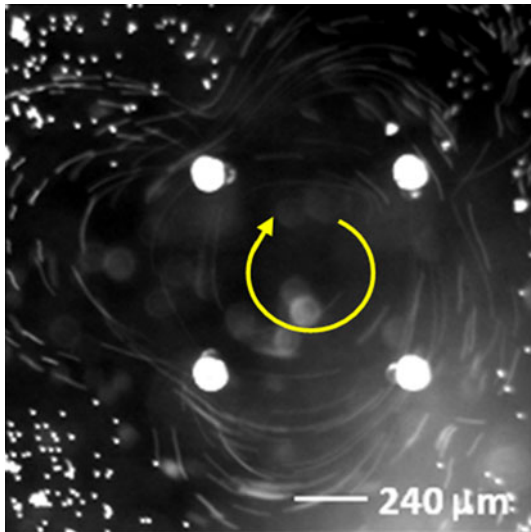


Fig. 5 The image shows the flow field developed around an array of four *teardrop-shaped* cavities with their respective tails pointing orthogonally to each other, causing the particles to be directed clockwise. The exposure time for the image is 190 ms

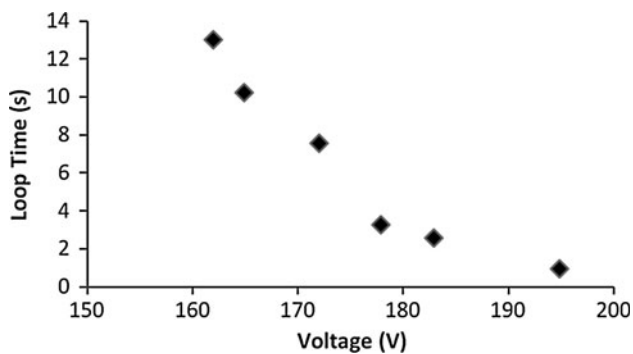


Fig. 6 The graph delineates the time it takes for the particle to move in a closed loop (along the *symmetry lines* of the cavities) measured against input voltage to the piezoelectric transducer; the parameters bear an inverse relation. A high voltage creates a higher flow speed and a shorter loop time, while a lower voltage induces a slower flow speed and a longer loop time

designed when perfectly made with the micro-milling machine. On one hand, although the bubble shape was found to be very repeatable, a marginal variation in bubble size will demand the actuation frequency to be fine-tuned. On the other hand, some testing factors lead to diminishing returns on repeated experiments. For one, the hole geometry is so important to the resultant bubble that any alterations to it will affect the microstreaming characteristics. The most common factor was a build-up of tracer particles used to visualize the microstreaming. While essential for observation, the particles eventually gather in the holes after several tests to the point of shoving out any trapped air and preventing any microstreaming. This problem can be mitigated by cleaning the chip in between experiments

or eliminating the particles altogether in future experiments. Another error factor is “random bubbles” or accidentally trapped air on the chip. These bubbles can oscillate and cause unintended microstreaming. In our experiments, these bubbles were manually removed with a needle. Possible solutions in the future include hydrophobicity control of the substrate (Betz et al. 2010; Drelich et al. 2011) and implementation of bubble removal elements (Xu et al. 2010; Liu et al. 2011).

4 Conclusion

In this communication, we have presented our preliminary results on an innovative active flow control method in a microfluidic environment using acoustically activated microbubbles confined in teardrop-shaped cavities. We have shown how the dimensions and orientation of teardrop-shaped cavities are essential to precise bubble confinement, the direction of the flow field, and the streaming frequency of the trapped bubble. Utilizing these design parameters, we have displayed frequency-selective excitation of two different-sized microbubbles in creating a flow switch. In a third set of experiments we used a square array of teardrop-shaped cavities to direct flow in a loop. We plan to build complicated flow circuits and perform precise measurements in our follow-up studies. We believe that teardrop cavities have great potential in microfluidic devices for enhancing flow control both spatially and temporally and providing alternatives to micropumps and fixated micro-transporters.

Acknowledgments This research is supported by DARPA Young Faculty Award N66001-11-1-4127 and WSUV Faculty Research Mini-Grant.

References

- Ahmed D, Mao XL, Juluri BK, Huang TJ (2009a) A fast microfluidic mixer based on acoustically driven sidewall-trapped microbubbles. *Microfluid Nanofluid* 7(5):727–731
- Ahmed D, Mao XL, Shi JJ, Juluri BK, Huang TJ (2009b) A millisecond micromixer via single-bubble-based acoustic streaming. *Lab Chip* 9(18):2738–2741
- Betz A, Xu J, Qiu H, Attinger D (2010) Do surfaces with mixed hydrophilic and hydrophobic areas enhance pool boiling? *Appl Phys Lett* 97:141909
- Chung SK, Cho SK (2008) On-chip manipulation of objects using mobile oscillating bubbles. *J Micromech Microeng* 18:12
- Chung SK, Cho SK (2009) 3-D manipulation of millimeter- and micro-sized objects using an acoustically excited oscillating bubble. *Microfluid Nanofluid* 6(2):261–265
- Drelich J, Chibowski E, Meng DD, Terpilowski K (2011) Hydrophilic and superhydrophilic surfaces and materials. *Soft Matter* 7(21):9804

- Elder SA (1959) Cavitation microstreaming. *J Acoust Soc Am* 31(1):11
- Garty G, Grad M, Jones BK, Xu Y, Xu J, Randers-Pehrson G, Attinger D, Brenner DJ (2011) Design of a novel flow-and-shoot microbeam. *Radiat Prot Dosim* 143(2–4):344–348
- Hashmi A, Yu G, Reilly-Collette M, Heiman G, Xu J (2012a) Oscillating bubbles: a versatile tool for lab on a chip applications. *Lab Chip* 12(21):4216–4227
- Hashmi A, Yu G, Xu Y, Kwon HJ, Chen XL, Xu J (2012b) Microbubble array for on-chip worm processing (submitted)
- Hettiarachchi K, Lee AP (2010) Polymer–lipid microbubbles for biosensing and the formation of porous structures. *J Colloid Interf Sci* 344(2):521–527
- Hettiarachchi K, Zhang S, Feingold S, Lee AP, Dayton PA (2009) Controllable microfluidic synthesis of multiphase drug-carrying lipospheres for site-targeted therapy. *Biotechnol Prog* 25(4): 938–945
- Huang PH, Lapsley MI, Ahmed D, Chen Y, Wang L, Huang TJ (2012) A single-layer, planar, optofluidic switch powered by acoustically driven, oscillating microbubbles. *Appl Phys Lett* 101(14):141101
- Kao J, Wang XL, Warren J, Xu J, Attinger D (2007) A bubble-powered micro-rotor: conception, manufacturing, assembly and characterization. *J Micromech Microeng* 17(12):2454–2460
- Kwon JO, Yang JS, Lee SJ, Rhee K, Chung SK (2011) Electromagnetically actuated micromanipulator using an acoustically oscillating bubble. *J Micromech Microeng* 21:11
- Lee KH, Lee JH, Won JM, Rhee K, Chung SK (2011) Micromanipulation using cavitation microstreaming generated by acoustically oscillating twin bubbles. *Sensor Actuat A Phys*. doi: [10.1016/j.sna.2011.11.037](https://doi.org/10.1016/j.sna.2011.11.037)
- Leslie DC, Easley CJ, Seker E, Karlinsey JM, Utz M, Begley MR, Landers JP (2009) Frequency-specific flow control in microfluidic circuits with passive elastomeric features. *Nat Phys* 5(3):231–235
- Liu RH, Yang JN, Pindera MZ, Athavale M, Grodzinski P (2002) Bubble-induced acoustic micromixing. *Lab Chip* 2(3):151–157
- Liu C, Thompson JA, Bau HH (2011) A membrane-based, high-efficiency, microfluidic debubbler. *Lab Chip* 11(9):1688–1693
- Marmottant P, Hilgenfeldt S (2003) Controlled vesicle deformation and lysis by single oscillating bubbles. *Nature* 423(6936):153
- Marmottant P, Hilgenfeldt S (2004) A bubble-driven microfluidic transport element for bioengineering. *P Natl Acad Sci USA* 101(26):9523–9527
- Marmottant P, Raven JP, Gardeniers H, Bomer JG, Hilgenfeldt S (2006) Microfluidics with ultrasound-driven bubbles. *J Fluid Mech* 568:109–118
- Matsumoto K, Ueno I (2009) Oscillating bubbles in ultrasonic acoustic field. *J Phys Conf Ser* 147:012015
- Okabe Y, Chen Y, Purohit R, Corn RM, Lee AP (2012) Piezoelectrically driven vertical cavity acoustic transducers for the convective transport and rapid detection of DNA and protein binding to DNA microarrays with SPR imaging—A parametric study. *Biosens Bioelectron* 35(1):37–43
- Packer J, Attinger D, Ventikos Y (2008) Ultrasound-driven viscous streaming, modelled via momentum injection. *Sens Transducers J* 3:47–58
- Patel MV, Tovar AR, Lee AP (2012) Lateral cavity acoustic transducer as an on-chip cell/particle microfluidic switch. *Lab Chip* 12(1):139–145
- Rogers P, Neild A (2011) Selective particle trapping using an oscillating microbubble. *Lab Chip* 11(21):3710–3715
- Stone HA, Stroock AD, Ajdari A (2004) Engineering flows in small devices: microfluidics toward a lab-on-a-chip. *Annu Rev Fluid Mech* 36:381–411
- Tovar A, Patel M, Lee A (2011) Lateral air cavities for microfluidic pumping with the use of acoustic energy. *Microfluid Nanofluid* 10(6):1269–1278
- Wang Z, Zhe J (2011) Recent advances in particle and droplet manipulation for lab-on-a-chip devices based on surface acoustic waves. *Lab Chip* 11(7):1280–1285
- Wang XL, Attinger D, Moraga F (2006) A micro-rotor driven by an acoustic bubble. *Nanosc Microsc Therm* 10(4):379–385
- Wang C, Jalikop SV, Hilgenfeldt S (2011a) Size-sensitive sorting of microparticles through control of flow geometry. *Appl Phys Lett* 99:3
- Wang SS, Huang XY, Yang C (2011b) Mixing enhancement for high viscous fluids in a microfluidic chamber. *Lab Chip* 11(12): 2081–2087
- Won JM, Lee JH, Lee KH, Rhee K, Chung SK (2011) *Int J Precis Eng Man* 12:577–580
- Xie Y, Ahmed D, Lapsley MI, Lin SC, Nawaz AA, Wang L, Huang TJ (2012) Single-shot characterization of enzymatic reaction constants k_m and k_{cat} by an acoustic-driven, bubble-based fast micromixer. *Anal Chem* 84(17):7495–7501
- Xu J, Attinger D (2007a) Acoustic excitation of superharmonic capillary waves on a meniscus in a planar microgeometry. *Phys Fluids* 19:108107
- Xu J, Attinger D (2007b) Control and ultrasonic actuation of a gas-liquid interface in a microfluidic chip. *J Micromech Microeng* 17(3):609–616
- Xu J, Attinger D (2008) Drop on demand in a microfluidic chip. *J Micromech Microeng* 18:065020
- Xu J, Vaillant R, Attinger D (2010) Use of a porous membrane for gas bubble removal in microfluidic channels: physical mechanisms and design criteria. *Microfluid Nanofluid* 9(4):765–772
- Yu G, Chen XL, Xu J (2011) Acoustophoresis in variously shaped liquid droplets. *Soft Matter* 7(21):10063–10069